# *In situ* enhancement of toughness of SiC–$TiB_2$ composites

KYEONG-SIK CHO, HEON-JIN CHOI, JUNE-GUNN LEE
*Division of Ceramics, Korea Institute of Science and Technology, PO Box 131, Cheongryang, Seoul 130-650, Korea*

YOUNG-WOOK KIM
*Department of Materials Science and Engineering, The University of Seoul, 90 Jeonnong-Dong, Seoul 130-743, Korea*

A process based on liquid phase sintering and subsequent annealing for grain growth is presented to obtain the *in situ* enhancement of toughness of SiC–30 wt %, 50 wt %, and 70 wt % $TiB_2$ composites. Its microstructures consist of uniformly distributed elongated α-SiC grains, relatively equiaxed $TiB_2$ grains, and yttrium aluminium garnet (YAG) as a grain boundary phase. The composites were fabricated from β-SiC and $TiB_2$ powders with the liquid forming additives of $Al_2O_3$ and $Y_2O_3$ by hot-pressing at 1850 °C and subsequent annealing at 1950 °C. The annealing led to the *in situ* growth of elongated α-SiC grains, due to the $\beta \rightarrow \alpha$ phase transformation of SiC, and the coarsening of $TiB_2$ grains. The fracture toughness of the SiC–50 wt % $TiB_2$ composites after 6 h annealing was 7.3 MPa $m^{1/2}$, approximately 60% higher than that of as-hot-pressed composites (4.5 MPa $m^{1/2}$). Bridging and crack deflection by the elongated α-SiC grains and coarse $TiB_2$ grains appear to account for the increased toughness of the composites.

## 1. Introduction

Composites of SiC–$TiB_2$ can be fabricated by hot pressing with the aid of C and Al or B [1, 2] or pressureless sintering with *in situ* synthesis of $TiB_2$ through a reaction between TiC and boron [3] to a near full density at temperatures in excess of 2000 °C. Several investigations have shown that the dispersion of $TiB_2$ particles results in the improved fracture toughness of SiC ceramics [3–5]. It is claimed that the residual stresses due to the thermal expansion mismatch between $TiB_2$ ($8.6 \times 10^{-6}\,°C^{-1}$) and SiC ($4.2 \times 10^{-6}\,°C^{-1}$) improve toughness by deflecting the cracks around the $TiB_2$ particles [2, 3].

Recently, several reports have been published on *in situ* toughened SiC [6–10], akin to $Si_3N_4$. The improvement of fracture toughness was achieved through the development of elongated α-SiC grains [7–11].

In this study, we present an alternative microstructural design for enhancing the fracture toughness of SiC–$TiB_2$ composites. We have used liquid phase sintering to fabricate SiC–30 wt %, 50 wt %, and 70 wt % $TiB_2$ composites at relatively low temperature (1850 °C) [12], and subsequent annealing at 1950 °C to develop the *in situ* growth of elongated α-SiC grains as well as coarse $TiB_2$ grains. The fracture toughness and strength of the composites were presented as a function of $TiB_2$ content and annealing time.

## 2. Experimental procedure

Commercially available β-SiC (Ibiden Co., Ltd, Nagoya, Japan, grade Ultrafine), $TiB_2$ (H.C. Starck, Berlin, Germany, grade F), $Al_2O_3$ (Sumitomo Chemicals, Tokyo, Japan, grade AKP-30), and $Y_2O_3$ powders (H.C. Starck, Berlin, Germany, grade Fine) were used as the starting powders. The powder mixtures of 90 wt % β-SiC with 7 wt % $Al_2O_3$ and 3 wt % $Y_2O_3$ for monolithic SiC, and the powder mixtures of SiC–$TiB_2$ containing 30–70 wt % $TiB_2$ with 7 wt % $Al_2O_3$ and 3 wt % $Y_2O_3$ for SiC–$TiB_2$ composites were ball milled in ethanol with SiC grinding balls for 24 h. The milled slurry was dried and sieved through a 60 mesh screen. The granulated powders were hot pressed in a graphite resistance furnace at 1850 °C for 1 h at 25 MPa to final dimensions of 30 mm in diameter by 20 mm high. The hot-pressed SiC–$TiB_2$ composites were subsequently heat treated at 1950 °C for 6 and 12 h under flowing argon in the same furnace without pressure to enhance the grain growth of $TiB_2$ and the $\beta \rightarrow \alpha$ phase transformation of SiC.

Densities of composites prepared by grinding off the surface layers were measured using the Archimedes method and the relative densities of the specimens were calculated based on the densities of SiC (3.215 g $cm^{-3}$), $TiB_2$ (4.495 g $cm^{-3}$), $Al_2O_3$ (3.987 g $cm^{-3}$), and $Y_2O_3$ (5.031 g $cm^{-3}$) assuming a rule of mixtures. Crystalline phases in the sintered specimens were determined by X-ray diffractometry

0022–2461  

(XRD). The microstructure was observed by scanning electron microscopy (SEM) for polished specimens. Some specimens were polished up to 1 μm diamond paste and plasma etched for observing grain size of SiC. The grain sizes of equiaxed grains, i.e. SiC in monolithic SiC and as-hot-pressed composites and $TiB_2$ in as-hot-pressed and annealed composites, were determined from the diameter of circle approximation with equivalent area in its two-dimensional image. However, the length and diameter of SiC grains in annealed composites, which have mostly elongated shapes, were determined from the longest and the shortest grain diagonals, respectively, in its two-dimensional image. A total of 300–500 grains was used for the statistical analysis of each specimen. The hot-pressed and annealed specimens were also cut and machined into $3 \times 4 \times 25$ mm bars with an 80 grit diamond wheel for flexural testing. Bend tests were performed at room temperature on six specimens for each condition using a four-point method with outer and inner spans of 20 and 8 mm, respectively, at a crosshead speed of 0.5 mm $min^{-1}$. The fracture toughness was estimated by measuring crack lengths generated by a Vicker's indenter with a load of 196 N. The following equation, proposed by Anstics *et al.* [13], was used for the calculation

$$K_c = \S_v \left(\frac{E}{H}\right)^{1/2} P(c^{-3/2})$$

Here $\S_v$ is a material-independent constant for Vicker's-produced radial crack; $\S_v = 0.016$ was used in the present study. $E$, $H$, $P$ and $c$ represent Young's modulus, the Vicker's hardness, the indentation load and the half-length of radial crack, respectively. Young's moduli of SiC–$TiB_2$ composites were calculated from the Young's moduli of SiC (450 GPa) and $TiB_2$ (529 GPa), assuming a rule of mixture.

## 3. Results and discussion

The characteristics of the monolithic SiC and the SiC–$TiB_2$ composites are summarized in Table I. The relative densities of $\geqslant 97\%$ were achieved by hot-pressing with a holding time of 1 h at 1850 °C. However, prolonged annealing at 1950 °C resulted in the decrease of relative density, probably because of the formation of volatile components such as AlO, $Al_2O$ and CO [14]. Phase analysis of hot-pressed specimens by XRD showed β-SiC, YAG and α-$Al_2O_3$ for monolithic SiC and β-SiC, $TiB_2$, YAG and α-$Al_2O_3$ for SiC–$TiB_2$ composites. In contrast, annealed specimens of the composites were found to be composed of α-SiC, $TiB_2$ and YAG. Polytype of the α-SiC was identified as 4H. It indicated that the $\beta \rightarrow \alpha$ phase transformation had occurred and α-$Al_2O_3$ had volatilized via reactions among SiC, $TiB_2$ and $Al_2O_3$ during annealing.

Fig. 1 shows the microstructure of monolithic SiC and SiC–30 wt % $TiB_2$ composite after hot pressing. Pore-like grains in Fig. 1b are $TiB_2$ grains removed by plasma etching. As shown, the monolithic SiC was composed mostly of equiaxed grains with average size of 0.54 μm, as shown in Table I. The SiC–$TiB_2$ composite was a two-phase particulate composite consisting of randomly distributed $TiB_2$ grains (grain size of $\sim 1.71$ μm) in the relatively fine SiC matrix (grain size of 0.58 μm). The size and shape of SiC grains in SiC–30 wt % $TiB_2$ composites (Fig. 1b) were almost the same with those of monolithic SiC (Fig. 1a), indicating the $TiB_2$ grains did not work as a grain growth inhibitor of SiC.

Figs 2 and 3 show the microstructural change of the composites with annealing time. The bright grey phase is $TiB_2$, the dark grey phase is SiC, and white phase is oxide additives, presumably YAG. The effect of annealing became apparent after 6 h, as shown in Fig. 2b and Fig. 3b that indicate, referring to the phase and image analyses in Table I, the marked growth of α-SiC. The length and diameter of SiC grains in the composites increased gradually with annealing time, as shown in Table I. It indicates that the grain growth and $\beta \rightarrow \alpha$ phase transformation of SiC took place simultaneously during annealing. The average aspect ratio of SiC grains decreased, i.e. from 4.1 for 12-h annealed SiC–30 wt % $TiB_2$ composite to 2.6 for 12-h

TABLE I Properties of monolithic SiC and SiC–$TiB_2$ composites

| Composition (wt%) | | | | Annealing time at 1950 °C (h) | Relative density (%) | Crystalline phase | | SiC grain | | $TiB_2$ grain size (μm) | Fracture toughness (MPa $m^{1/2}$) | Flexural strength (MPa) |
|---|---|---|---|---|---|---|---|---|---|---|---|---|
| SiC | $TiB_2$ | $Al_2O_3$ | $Y_2O_3$ | | | Major | Trace | Aspect ratio | Length × diameter (μm) | | | |
| 90 | – | 7 | 3 | 0 | 99.4 | β-SiC | YAG[a], α-$Al_2O_3$ | | 0.54[b] | – | 3.6±0.4 | 611±42 |
| 60 | 30 | 7 | 3 | 0 | 97.4 | β-SiC, $TiB_2$ | YAG, α-$Al_2O_3$ | | 0.58[b] | 1.71 | 4.4±0.5 | 571±39 |
| | | | | 6 | 96.8 | α-SiC, $TiB_2$ | YAG | 3.9 | 7.73 × 2.00 | 2.44 | 6.7±0.4 | 550±33 |
| | | | | 12 | 95.5 | α-SiC, $TiB_2$ | YAG | 4.1 | 8.49 × 2.07 | 2.59 | 6.4±0.4 | 501±39 |
| 40 | 50 | 7 | 3 | 0 | 97.2 | β-SiC, $TiB_2$ | YAG, α-$Al_2O_3$ | | 0.60[b] | 2.00 | 4.5±0.4 | 504±33 |
| | | | | 6 | 97.0 | α-SiC, $TiB_2$ | YAG | 3.0 | 7.54 × 2.51 | 4.13 | 7.3±0.5 | 389±32 |
| | | | | 12 | 96.4 | α-SiC, $TiB_2$ | YAG | 3.1 | 8.38 × 2.73 | 5.56 | 7.1±0.4 | 290±29 |
| 20 | 70 | 7 | 3 | 0 | 98.3 | β-SiC, $TiB_2$ | YAG, α-$Al_2O_3$ | | 0.62[b] | 3.70 | 4.1±0.5 | 593±38 |
| | | | | 6 | 97.3 | α-SiC, $TiB_2$ | YAG | 2.5 | 7.34 × 2.88 | 5.94 | 6.8±0.6 | 332±32 |
| | | | | 12 | 97.0 | α-SiC, $TiB_2$ | YAG | 2.6 | 8.36 × 3.21 | 6.89 | 6.9±0.5 | 231±31 |

[a]$Al_5Y_3O_{12}$ (yttrium aluminium garnet).
[b]Average grain size.

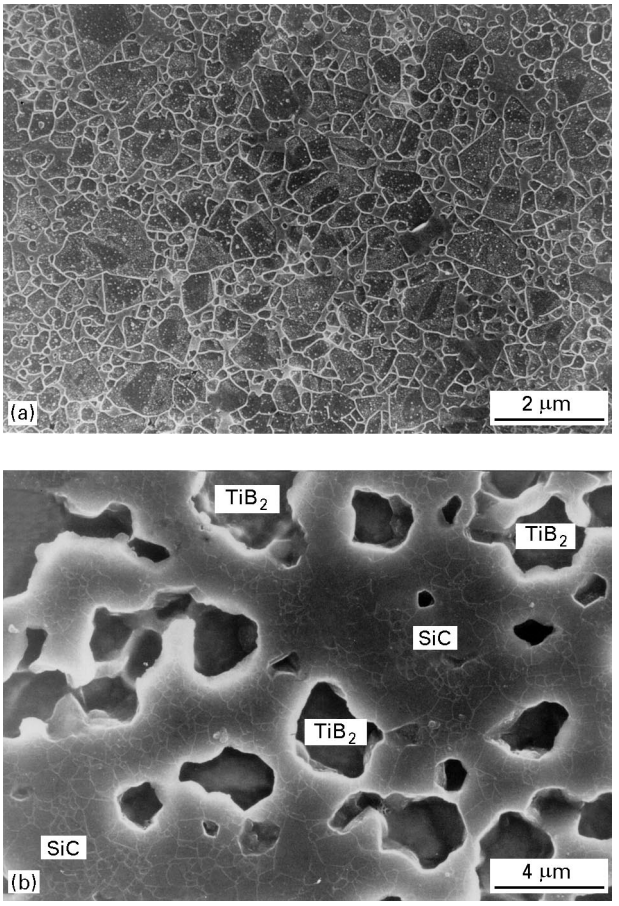


*Figure 1* SEM micrographs of as-hot-pressed materials: (a) monolithic SiC and (b) SiC–30 wt % $TiB_2$ composites. (The $TiB_2$ grains were removed from the surface by the plasma etching.)

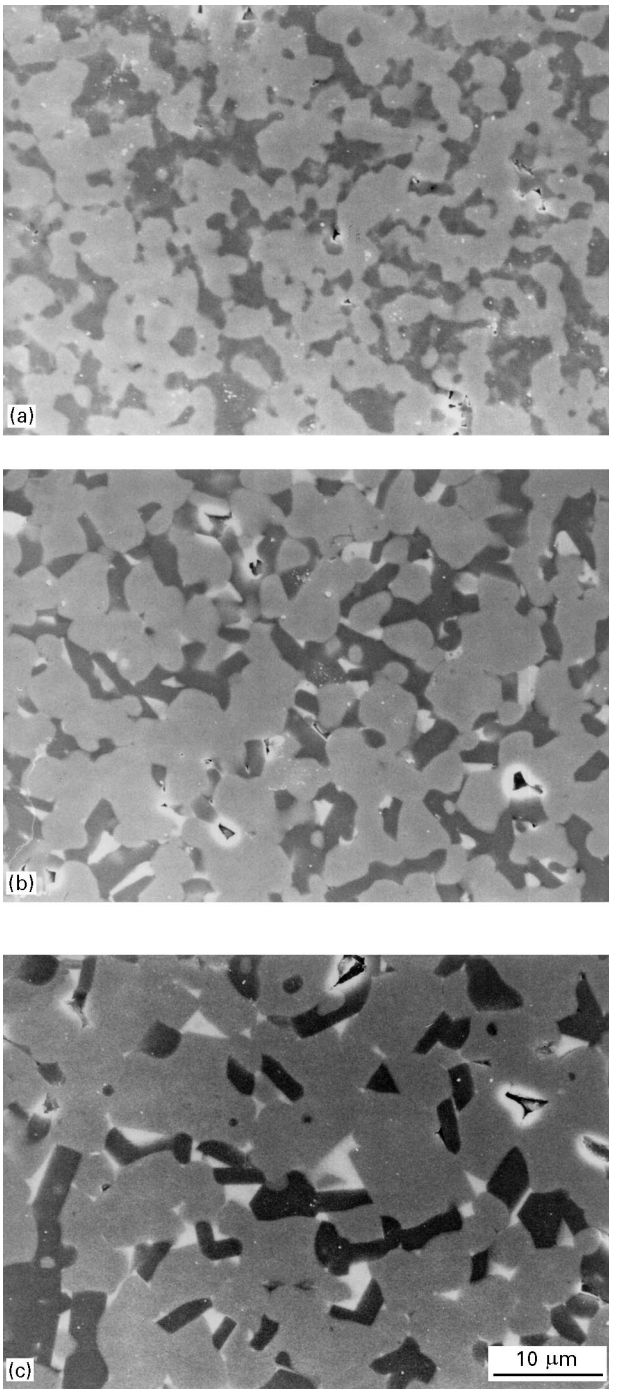


*Figure 2* SEM micrographs of polished cross sections of (a) as-hot-pressed SiC–70 wt % $TiB_2$ composites, and annealed at 1950 °C for (b) 6 h and (c) 12 h.

annealed SiC–70 wt % $TiB_2$ composite, with increasing the amount of $TiB_2$ in the composites. It indicates that the anisotropy in the grain shape of SiC grains decreases with increasing the $TiB_2$ content in the composites. Another interesting feature is the grain coarsening of $TiB_2$ during annealing, e.g. whose diameters increased from 3.70 to 6.89 μm for SiC–70 wt % $TiB_2$ composites.

The effect of annealing time on the fracture toughness of SiC–$TiB_2$ composites is also shown in Table I. The fracture toughness of monolithic SiC was measured as a reference. The fracture toughness increased with increasing annealing time and showed the maximum of 7.3 MPa $m^{1/2}$ at 6 h for SiC–50 wt % $TiB_2$ composites. This value is approximately 60% higher than that of as-hot-pressed composites (4.5 MPa $m^{1/2}$). The increase in fracture toughness after 6-h annealing was considered to be due to the enhanced bridging and crack deflection by the elongated α-SiC grains as well as coarse $TiB_2$ grains, as shown in Fig. 3. It is well documented that the grain coarsening in particulate composites leads to the increased fracture toughness, owing to the enhanced crack deflection [15–18]. Further annealing up to 12 h, however, decreased the fracture toughness slightly, although the lengths and widths of α-SiC and $TiB_2$ grains were increased. This could be attributed to the increasing tendency of transgranular fracture and pore formation with the prolonged annealing. This phenomenon is quite similar to the *in situ* toughened SiC–TiC composites [19]. Table I also shows that the hot-pressed materials, which were composed of relatively fine grains, have relatively low fracture toughness (4.1–4.5 MPa $m^{1/2}$) and relatively high flexural strength (504–593 MPa). In contrast, 6-h annealed materials, which were composed of relatively large elongated SiC grains and coarse $TiB_2$ grains, have relatively high fracture toughness (6.7–7.3 MPa $m^{1/2}$) and relatively low flexural strength (332–550 MPa). The marked growth of both the elongated α-SiC and $TiB_2$ grains with increasing the annealing time resulted in the improved fracture toughness and decreased strength. Thus, coarse, *in situ*

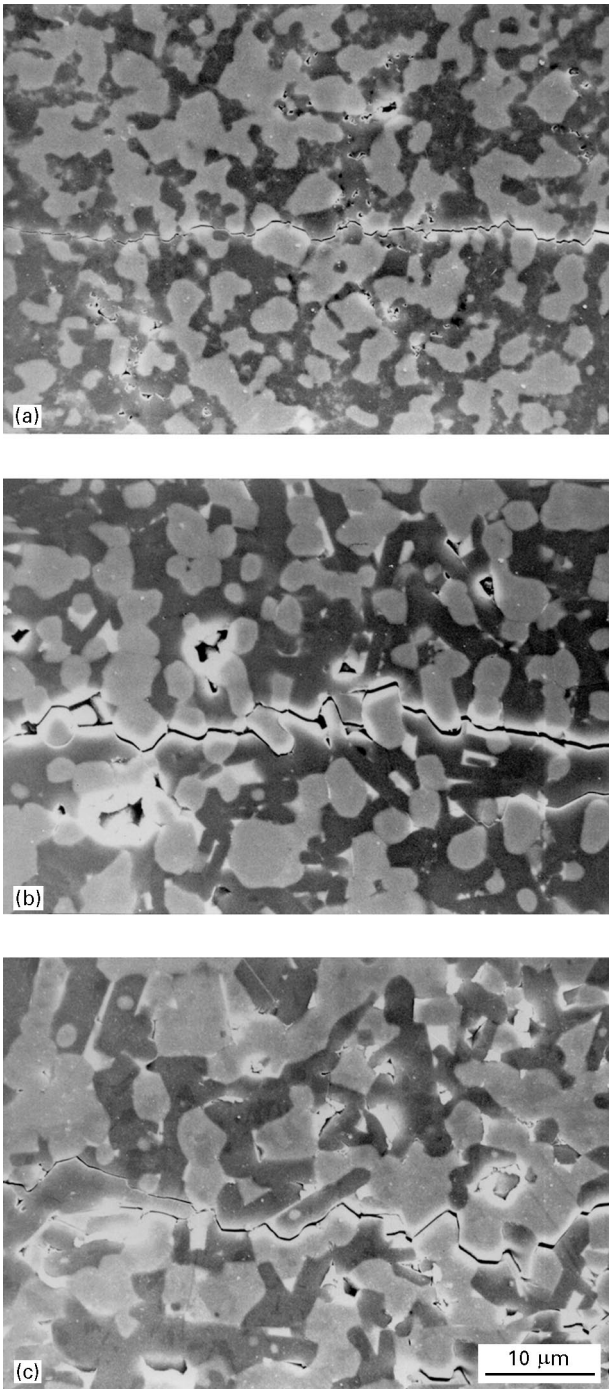


*Figure 3* SEM micrographs of a crack path induced by a Vicker's indenter for (a) as-hot-pressed SiC–50 wt % $TiB_2$ composite, and annealed at 1950 °C for (b) 6 h and (c) 12 h.

toughened microstructure of annealed material is beneficial to the toughness. On the other hand, fine, equiaxed microstructure of hot-pressed material is beneficial to the strength. From the above results, we can conclude that the improved toughness is offset by a significant reduction in strength.

## 4. Summary

*In situ* enhancement of toughness of SiC–$TiB_2$ composites with microstructures consisting of uniformly distributed elongated α-SiC grains, relatively equiaxed $TiB_2$ grains, and YAG as a grain boundary phase were fabricated from β-SiC and $TiB_2$ powders with the liquid forming additives of $Al_2O_3$ and $Y_2O_3$. By hot-pressing and subsequent annealing, elongated α-SiC was grown via the $\beta \rightarrow \alpha$ phase transformation and the relatively coarse $TiB_2$ grains were grown by the grain growth. The fracture toughness of the SiC–50 wt % $TiB_2$ composites after 6-h annealing was as high as 7.3 MPa $m^{1/2}$, because of the bridging and crack deflection by the elongated α-SiC grains and coarse $TiB_2$ grains. However, the improved toughness is offset by a significant reduction in strength.

## References

1. M. A. JANNEY, *Am. Ceram. Soc. Bull.* **66** (1987) 322.
2. Y. W. KIM, H. J. CHOI, J. G. LEE, S. W. LEE and S. K. CHUNG, *Kor. J. Ceram* **1** (1995) 125.
3. Y. OHYA, M. J. HOFFMANN and G. PETZOW, *J. Am. Ceram. Soc.* **75** (1992) 2479.
4. C. H. McMURTRY, W. D. G. BOECKER, S. G. SESHADRI, J. S. ZANGHI and E. GARNIER, *Am. Ceram. Soc. Bull.* **66** (1987) 325.
5. T. TANI and S. WADA, *J. Mater. Sci.* **25** (1990) 157.
6. Y. W. KIM, M. MITOMO and H. HIROTSURU, *J. Am. Ceram. Soc.* **78** (1995) 3145.
7. N. P. PADTURE, *ibid.* **77** (1994) 519.
8. N. P. PADTURE and B. R. LAWN, *ibid.* **77** (1994) 2518.
9. V. D. KRISTIC, *Mater. Res. Soc. Bull.* **20** (1995) 46.
10. S. K. LEE and C. H. KIM, *J. Am. Ceram. Soc.* **77** (1994) 1655.
11. M. A. MULLA and V. D. KRSTIC, *Acta Metall. Mater.* **42** (1994) 303.
12. K. S. CHO, Y. W. KIM, H. J. CHOI and J. G. LEE, *J. Mater. Sci.* **31** (1996) 6223.
13. G. R. ANSTICS, P. CHANTIKUL, B. R. LAWN and D. B. MARSHALL, *J. Am. Ceram. Soc.* **64** (1981) 533.
14. Y. W. KIM, H. TANAKA, M. MITOMO and S. OTANI, *J. Ceram. Soc. Jpn* **103** (1995) 257.
15. R. W. RICE, S. W. FREIMAN and P. F. BECHER, *J. Am. Ceram. Soc.* **64** (1981) 345.
16. *Idem., ibid.* **64** (1981) 350.
17. B. MUSSLER, M. V. SWAIN and N. CLAUSSEN, *ibid.* **65** (1982) 566.
18. P. L. SWANSON, C. J. FAIRBANKS, B. R. LAWN and Y. W. MAI, *ibid.* **70** (1987) 279.
19. K. S. CHO, Y. W. KIM, H. J. CHOI and J. G. LEE, *ibid.* **79** (1996) 1711.

*Received 7 May 1996*
*and accepted 24 July 1997*